Uranium isotopes fingerprint biotic reduction

Malgorzata Stylo[a], Nadja Neubert[b], Yuheng Wang[a], Nikhil Monga[c], Stephen J. Romaniello[c], Stefan Weyer[b], and Rizlan Bernier-Latmani[a,1]

[a]Environmental Microbiology Laboratory, École Polytechnique Fédérale de Lausanne, CH-1015 Lausanne, Switzerland; [b]Institut für Mineralogie, Leibniz Universitat Hannover, D-30167 Hannover, Germany; and [c]School of Earth and Space Exploration, Arizona State University, 85287 Tempe, AZ

Edited by Donald E. Canfield, Institute of Biology and Nordic Center for Earth Evolution, University of Southern Denmark, Odense M., Denmark, and approved March 23, 2015 (received for review November 17, 2014)

Knowledge of paleo-redox conditions in the Earth's history provides a window into events that shaped the evolution of life on our planet. The role of microbial activity in paleo-redox processes remains unexplored due to the inability to discriminate biotic from abiotic redox transformations in the rock record. The ability to deconvolute these two processes would provide a means to identify environmental niches in which microbial activity was prevalent at a specific time in paleo-history and to correlate specific biogeochemical events with the corresponding microbial metabolism. Here, we demonstrate that the isotopic signature associated with microbial reduction of hexavalent uranium (U), i.e., the accumulation of the heavy isotope in the U(IV) phase, is readily distinguishable from that generated by abiotic uranium reduction in laboratory experiments. Thus, isotope signatures preserved in the geologic record through the reductive precipitation of uranium may provide the sought-after tool to probe for biotic processes. Because uranium is a common element in the Earth's crust and a wide variety of metabolic groups of microorganisms catalyze the biological reduction of U(VI), this tool is applicable to a multiplicity of geological epochs and terrestrial environments. The findings of this study indicate that biological activity contributed to the formation of many authigenic U deposits, including sandstone U deposits of various ages, as well as modern, Cretaceous, and Archean black shales. Additionally, engineered bioremediation activities also exhibit a biotic signature, suggesting that, although multiple pathways may be involved in the reduction, direct enzymatic reduction contributes substantially to the immobilization of uranium.

uranium | isotopes | paleoredox | biosignature | bioremediation

The search for a tool to discriminate biotic from abiotic processes principally triggered the investigation of isotope fractionation of metals through redox processes (1). Several prerequisites must be fulfilled in order for the isotope fractionation of a metal to represent an appropriate redox biosignature: (*i*) the geochemistry of the metal must include at least one biologically catalyzed reaction (e.g., biological oxidation or reduction); (*ii*) the transformation must result in immobilization of the metal and its isotopic fractionation; (*iii*) there must be a difference in isotopic signature between biotic and abiotic transformation; and (*iv*) the reaction must not go to completion (as quantitative conversion of reactants to product suppresses isotopic fractionation).

As demonstrated in this study, the radionuclide uranium (U) fulfills these requirements. Its mobility and deposition in low-temperature environments is controlled by redox transitions (2). The oxidized form [U(VI)] is largely soluble in the aqueous phase, whereas the reduced form [U(IV)] is sparingly soluble and precipitates, leading to U deposition under reducing conditions (3, 4). There are numerous pathways for U(VI) reduction, including direct biotic transformation mediated by metabolically varied microorganisms such as sulfate-reducing, iron-reducing, and fermenting bacteria (2), as well as abiotic reduction by redox-active minerals and solutes such as Fe(II)- or sulfide-bearing minerals, aqueous Fe(II), and sulfide species, as well as organic compounds (5–7).

Moreover, permil-level fractionations of the two abundant and primordial uranium isotopes are reported in association with U(VI) to U(IV) redox transitions through the accumulation of the heavy isotope (^{238}U) rather than the light isotope (^{235}U) in the reduced product (8–13). This isotopic signature has been measured in low-temperature paleo-environments, enabling the use of U isotope fractionation as a proxy for the redox conditions of ancient atmosphere and oceans (14–16). A recent study (17) observed enrichment of the heavier ^{238}U isotope in the products of biogenic U reduction, consistent with findings in nature (8, 10, 11, 18) and in agreement with ab initio calculations (19, 20).

Hence, the major remaining question is whether biotic reduction of U results in an exclusive and distinct isotopic signature, readily distinguishable from that generated by abiotic reduction. Here, we show that uranium isotope fractionation discriminates readily between biotic and abiotic reduction reactions through the major environmentally relevant pathways and propose the ^{238}U/^{235}U isotope ratio as a new bio-proxy for ancient and modern environments.

Results

U(VI) Reduction. To delineate the contribution of biotic and abiotic pathways to U isotopic fractionation, we systematically investigated changes in ^{238}U/^{235}U isotope ratios during biotic and abiotic U reduction using a laboratory-based approach (Fig. S1). Biotic U(VI) reduction by the metal-reducing bacterium *Shewanella oneidensis* strain MR-1 was examined under various culture conditions (Table S1). In addition, we conducted U(VI) reduction experiments using redox-active enzymes prepared

Significance

Throughout Earth's history, redox transformations in sedimentary environments have occurred through chemical processes (abiotic pathways) or via the activity of living microorganisms (biotic pathway). Tools able to discriminate between these two mechanisms are of major interest, as they would contribute significantly to the understanding of biogeochemical events that shaped the evolution of life on our planet. Here, we show that there is a clear difference between the isotopic signature associated with abiotic and biotic transformations of uranium (U). Thus, U isotopic composition can serve as a marker for biological processes in many sedimentary rocks. Based on this result, we conclude that microbial activity has contributed to reductive sedimentary processes in many low-temperature redox-active terrestrial and marine environments.

Author contributions: S.J.R., S.W., and R.B.-L. designed research; M.S., N.N., Y.W., and N.M. performed research; N.N. contributed new reagents/analytic tools; M.S., N.N., Y.W., N.M., S.J.R., S.W., and R.B.-L. analyzed data; and M.S., S.J.R., S.W., and R.B.-L. wrote the paper.

The authors declare no conflict of interest.

This article is a PNAS Direct Submission.

Freely available online through the PNAS open access option.

[1]To whom correspondence should be addressed. Email: rizlan.bernier-latmani@epfl.ch.

This article contains supporting information online at www.pnas.org/lookup/suppl/doi:10.1073/pnas.1421841112/-/DCSupplemental.

ENVIRONMENTAL SCIENCES

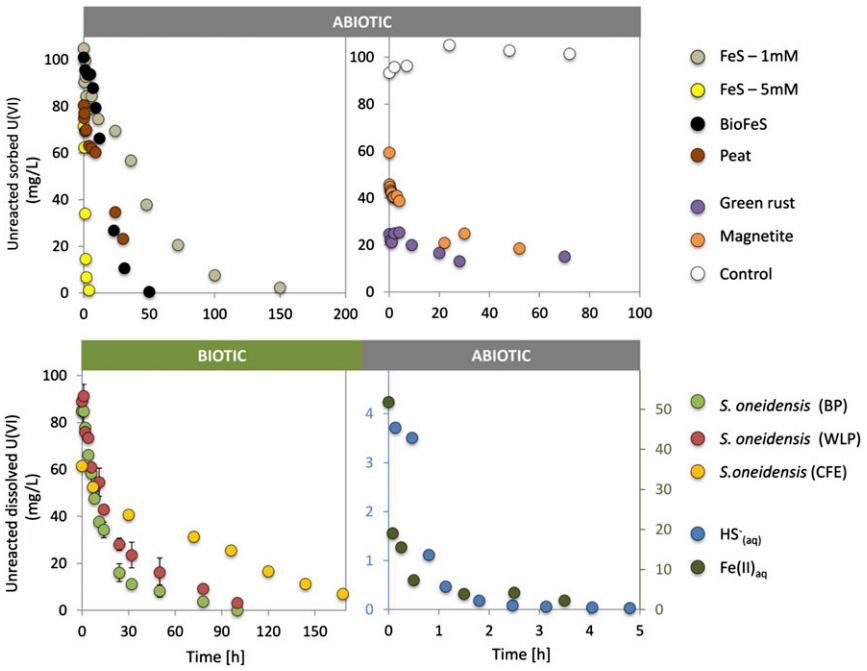

Fig. 1. U(VI) reduction for the various conditions considered: biologically mediated reduction by *S. oneidensis* in BP, WLP, or CFE; FeS- and peat-mediated reduction, magnetite or green-rust mediated reduction, and dissolved Fe(II)- and sulfide-mediated reduction. The controls represent cell-free experiments, where U(VI) was incubated with the Fe(III) mineral ferrihydrite. The *y* axis for abiotic samples [except aqueous Fe(II) and sulfide] correspond to unreacted U(VI) that is associated with the solid phase (sorbed). The *y* axis for biotic samples and Fe(II) and HS^- corresponds to unreacted dissolved U(VI). (*Lower Right*) Left *y* axis corresponds to unreacted dissolved U(VI) concentration [mg/L] for sulfide-mediated reduction and the right *y* axis to unreacted dissolved U(VI) concentration [mg/L] for Fe(II)-mediated reduction.

from a cell-free extract (CFE) of the same bacterium to isolate the role of cellular transport vs. that of redox active enzymes (21) in controlling biological U isotope fractionation (Fig. S2). We also investigated U(VI) reduction by a wide variety of environmental abiotic U(VI) reductants, including Fe-based reductants [magnetite, green rust, $Fe(II)_{aq}$], sulfur-based reductants (chemogenic and biogenic mackinawite [FeS (Figs. S3 and S4), bioFeS], aqueous sulfide), and reduced organic species (peat). In general, we found that the kinetics of biotic and abiotic U(VI) reduction proceeded at comparable rates. Only aqueous sulfide and ferrous iron exhibited more rapid reduction kinetics (Fig. 1).

Characterization of U(IV) Products. We used X-ray absorption spectroscopy to confirm the extent of U reduction and to characterize solid phase U reaction products (Table S2). Fig. 2 presents the extended X-ray absorption spectroscopy fine structure (EXAFS) spectra at the U L_{III}-edge for the final solid-phase U experimental products, as well as that of three reference spectra: U(VI) adsorbed onto the Fe(III) mineral ferrihydrite, crystalline UO_2, and a noncrystalline U(IV) species. By comparing reference spectra to those of the experimental products, we found that between 89% and 100% of the U end product was present as U(IV), providing direct proof of U reduction (Table S3) and ruling out the possibility of nonreductive precipitation or sorption of U(VI) species. In Fig. 2, the distinct speciation of U(IV)—either uraninite or noncrystalline U(IV)—is indicated by the presence/absence of the 3.8-Å peak in the Fourier-transformed EXAFS signal (22). These data demonstrate that uraninite (UO_2) was the primary U(IV) product of our abiotic reduction experiments, whereas noncrystalline U(IV) or a mixture of uraninite and noncrystalline U(IV) was produced during biological reduction experiments.

Isotopic Signature. The isotope composition of all experimental products, i.e., the remaining U(VI) fraction for all conditions and the corresponding U(IV) solid phase in selected cases, were measured by multicollector inductively coupled plasma (ICP)-MS using a double spike technique (9, 10). Isotope ratio measurements are reported in the standard delta notation relative to the initial experimental U stock (*SI Methods*).

For all biological reduction conditions, $\delta^{238}U$ values in the remaining dissolved U(VI) pool shift progressively toward more negative values, down to −2‰ (Fig. 3 and Table S4). These findings indicate preferential incorporation of ^{238}U into the reduced U(IV) species during biotic U reduction, in agreement with previous findings (17). They are further confirmed by the isotopic analysis of solid phase U(IV), showing a $\Delta^{238}U = 0.86 \pm 0.12$‰ between the U(IV) product and the remaining dissolved U(VI) (Fig. 4 and Table S5). We calculated an isotope fractionation factor α, and an enrichment factor ε, defined as

$$\varepsilon = 1{,}000‰ * (\alpha - 1),$$

by fitting the data to the Rayleigh distillation model (23). The resulting ε values are very similar for all biotic cases [and to previously published results (17)], i.e., ε = 0.85‰ (±0.08‰) when mostly crystalline U(IV) is formed [bicarbonate-Pipes medium (BP)], ε = 0.88‰ (±0.07‰) when mostly noncrystalline U(IV) is produced [Widdel low phosphate medium (WLP)], and ε = 0.85‰ (±0.04‰) for the CFE experiment. Thus, regardless of whether intact cells or cell-free extract containing cytochromes mediate the process, U reduction results in the preferential incorporation of ^{238}U into precipitated U(IV) species. These ε values also approach ab initio calculations predicting an equilibrium isotope fractionation of ε = 0.95‰ (20) and an experimental study reporting a value of ε = 1.40‰ (24).

In contrast to enzymatic U reduction, abiotic experiments, mediated by solid-phase or soluble reductants, exhibit either no U isotope fractionation or significant fractionation opposite in direction to that observed for biotic U reduction (Fig. 3 and Tables S4–S6). For reduction with chemogenic FeS, biogenic FeS, or peat, the $\delta^{238}U$ values of remaining U(VI) are, on average, similar to the starting composition, indicating little to no fractionation. Aqueous sulfide exhibits transient U isotope fractionation (accumulation of the heavy isotope in the dissolved phase) that disappeared over time. For magnetite, green rust, and aqueous Fe(II), significant isotope fractionation is observed, consistently showing enrichment of heavy isotopes in the remaining U(VI).

Discussion

Mechanisms of U Isotope Fractionation. The results presented here clearly demonstrate differences in U isotope fractionation among

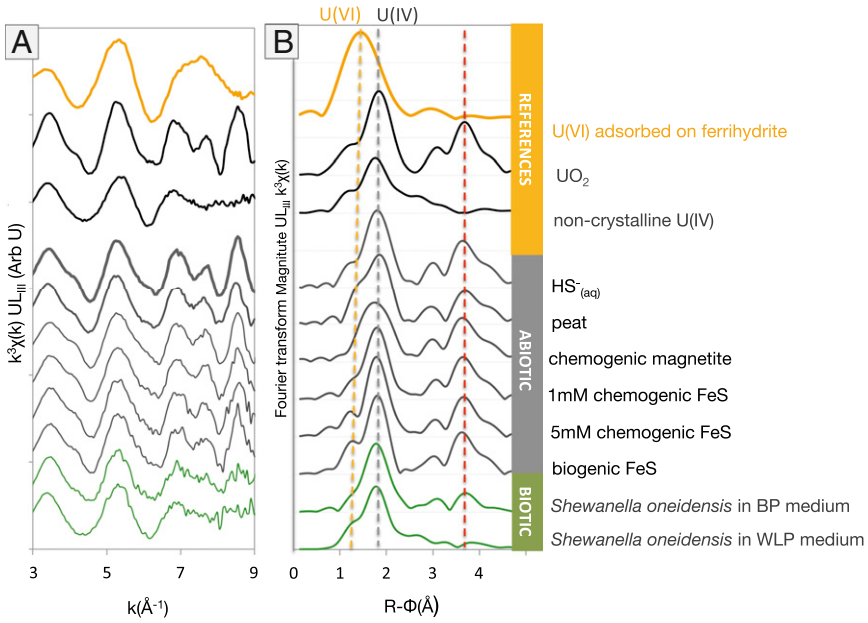

Fig. 2. EXAFS spectra (*A*) and the Fourier transform (*B*) of U products formed via biotic or abiotic reduction: strain MR-1 (in green) and mackinawite, magnetite, peat, or sulfide (in gray), as well as three reference spectra used for linear combination fits. Vertical lines in the Fourier transform panel correspond to the U-O pair correlation for U(VI) (yellow), U(IV) (gray), and the U-U pair correlation (red), indicating the presence of uraninite. The predominance of uraninite in abiotic systems is evidenced by the greater amplitude of the U-U shell relative to biotic systems.

the reduction pathways tested. Although more research will be needed to uncover the mechanistic details of the observed fractionation patterns, specific conclusions can be drawn from the current work.

The combination of our whole cell and CFE results suggests that, during biotic reduction, U(VI) uptake into the cell is not responsible for the observed isotope fractionation. Uranium reduction by *S. oneidensis* is catalyzed by multiheme *c*-type cytochromes localized on the outer membrane, the periplasm, and the cytoplasmic membrane (21). If isotope fractionation were dominantly generated during the transport of U(VI) across the outer membrane into the periplasm (i.e., if uptake by the cells were the rate-limiting step), the CFE condition would yield negligible isotope fractionation. However, isotope fractionation mediated by CFE was identical to that generated by intact cells, implying that the enzymatic transfer of electrons to U(VI) was likely responsible for $^{238}U/^{235}U$ fractionation.

Based on ab initio calculations (19, 20) and experimental work (24), the U(VI)/U(IV) equilibrium isotopic fractionation is expected to favor the heavy isotope in the U(IV) valence state. Indeed, for very heavy elements, such as U, isotope fractionation is dominated by a mass-independent fractionation mechanism. The nuclei of U isotopes differ in size and shape, and due to their large size, electron orbital energies are altered, leading to a phenomenon known as the nuclear field shift (19, 25). During reduction reactions, the added valence electrons are impacted by the nuclear field shift, resulting in varying energies of reaction for distinct isotopes. This difference in energetics of reduction causes isotopic fractionation. In the case of U, this mechanism results in isotope fractionation during equilibrium reactions that is opposite to the direction expected for traditional mass-dependent stable isotope fractionation (26).

During biotic U(VI) reduction, multiheme *c*-type cytochromes effect a one-electron transfer, resulting in the formation of U(V), which fractionates to U(VI) and U(IV) (2). The direction and magnitude of the observed U isotope fractionation are consistent with ab initio calculations and experimental values of equilibrium isotope fractionation (19, 20, 24, 27) even if full equilibrium may not be reached in the time frame of the experiments. Thus, when reduction occurs in the vicinity of the enzyme(s), the ^{238}U-favoring nuclear field shift effect dominates the fractionation behavior. Additionally, uranium isotopic fractionation was similar among bacterial species exhibiting distinct mechanisms and rates of U(VI) reduction (17). We propose that the biotic system may exhibit transient kinetic fractionation but that rapid isotopic exchange between U(VI) and U(IV) occurs in the vicinity of the enzyme, resulting in the near-equilibrium fractionation signature. This rapid exchange is possible in the biotic case because of the coexistence in the aqueous phase of U(VI) and small clusters of crystalline or labile noncrystalline U(IV) that form as a result of the reduction (22, 28). Thus, there is opportunity for the chemical interaction of aqueous U(VI) with small particles (a few atoms across) containing U(IV). This result is consistent with a recent study showing very rapid isotopic exchange between U(VI) and U(IV) when both species are in solution (27).

The mechanism of U(VI) reduction mediated by Fe(II)-bearing reducing agents remains controversial. It has been suggested to proceed via the transfer of a single electron to U(VI), producing U(V), followed by the disproportionation of U(V) to U(IV) and U(VI) (29, 30). However, there is also evidence that direct reduction to U(IV) occurs and is accompanied by the release of Fe(II) into solution (31). The discrepancy in reduction mechanisms observed among studies is likely due to the fact that control on the extent of U(VI) reduction is wrought by the combination of two competing factors: the Fe^{2+}/Fe^{3+} ratio at the surface of iron minerals and the U coordination environment (32).

For Fe(II)-bearing reducing agents, enrichment of ^{235}U is observed in the products of iron-mediated abiotic reduction. Isotope fractionation in this direction, opposite to that expected from equilibrium isotope fractionation, may indicate kinetic isotope effects. We suggest that nuclear field shift effects are muted or absent in the kinetics of these abiotic reduction reactions, resulting in the observed direction of fractionation.

Because mechanistic details of abiotic reduction with Fe(II)-bearing compounds are lacking, it is not possible to delineate the precise steps leading to isotopic fractionation in these systems. However, the data suggest that, in contrast to the biotic system, the fractionation generated by reduction processes persists in the product due to limited isotopic exchange between U(IV) and U(VI). Uranium in all three valences states [U(VI), U(V), and U(IV)] was reported to be sequestered at the surface or within the bulk of the Fe-bearing mineral (32, 33), precluding such exchange. This sequestration is also true for aqueous Fe(II)-mediated

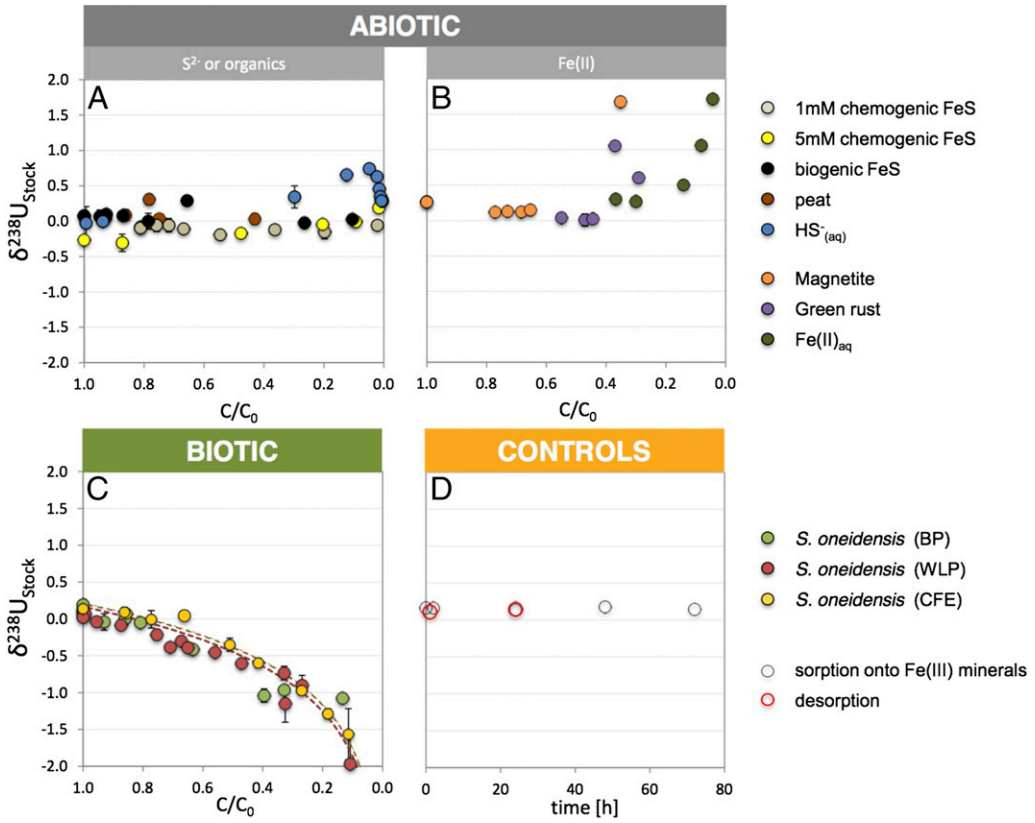

Fig. 3. $\delta^{238}U$ values for U(VI) plotted against the fraction of unreacted U(VI) during reduction by sulfide-containing or organic reductants (*A*) or Fe(II)-containing reductants for the abiotic system (*B*) and *S. oneidensis* for the biotic system (*C*). Reactions proceed from left to right. $\delta^{238}U$ values are plotted vs. time for control experiments (*D*). The continuous lines for the biotic experiments (with colors corresponding to the equivalent data set) represent the Rayleigh distillation model fit.

reduction due to the formation of an Fe(III)-bearing mineral as a result of the oxidation of Fe(II).

The lack of isotope fractionation for sulfide- or organic-mediated reduction may be attributed to direct two-electron transfer from organic matter or S^{2-} to U(VI), resulting in the sequestration of U(IV) and a strongly unidirectional reaction with insignificant isotope fractionation. The same lack of fractionation was observed in two other studies using reducing agents that operate via two-electron transfer: zerovalent iron by which Fe(0) transfers two electrons to U(VI) to form Fe(II) and U(IV) (34) and zerovalent zinc by which Zn^{2+} and U(IV) are produced (9).

Regardless of the exact reaction pathway, our results indicate that biological U reduction rapidly approaches predicted values for equilibrium isotope fractionation, whereas inorganic U reduction appears unable to obtain isotopic equilibrium, at least on experimental timescales. If preserved in the environment, the difference in isotopic fractionation during biotic vs. abiotic reduction would provide a much sought after isotopic biomarker for biologically mediated reductive processes.

Environmental Implications. A uranium isotope biomarker could be used to constrain the contribution of biotic U reduction in paleoredox studies, in remediation studies, and during the formation of natural ore deposits. Qualitatively, it can facilitate the determination of whether enzymatic processes contributed to the overall sequestration of U(IV). For example, a study of bioremediation at a U-contaminated site in Rifle (Colorado) via the amendment of acetate as an electron donor reported the enrichment of the light U isotopes in the remaining U(VI) pool in the groundwater as U reduction proceeded (18). This report suggests that microbial U reduction, i.e., the direct enzymatic pathway, played an important role in the generation of the observed U isotope fractionation in the aquifer. A more recent field-based study at the same uranium-contaminated site (35) suggested that U immobilization was due to biomass-associated mackinawite that acts as an electron source to reduce U(VI) to U(IV). However, according to the isotope signature of the process and the present findings, biogenic mackinawite could not have acted exclusively as a reducing agent in field-stimulated bioremediation. Rather, the extent of the reported U isotope fractionation (ε factor of 0.46‰) (18) compared with our experimental results for enzymatic U reduction (maximum ε factor of 0.88 ±0.07‰) suggest a combined biotic–abiotic pathway for U(VI) reduction in the subsurface.

Moreover, the measurement of $\delta^{238}U$ was proposed as an alternative tool for the assessment of U remediation progress in the field, where shifting isotopic ratios would be an indication of the active U immobilization, producing a result independent of complications such as adsorption and dilution effects (18). Results from this study allow the refinement of this tool to only target biologically mediated U(VI)-U(IV) redox transitions in the subsurface.

Geological Implications. Low-temperature ore deposits, such as sedimentary U deposits, require U(VI)-bearing fluids to react with a reduced zone, leading to the precipitation of U(IV) minerals (8, 36). In addition, moderate authigenic U enrichment is found in a range of geological settings, including marine sediments that formed under anoxic conditions. The latter include organic-rich sediments from recent anoxic or euxinic (anoxic with free H_2S in the water column) basins, such as the Black Sea or sediments formed in Archean times (15). All of these authigenically enriched U deposits show enrichment of $\delta^{238}U$, which is typically attributed to the U(VI)–U(IV) redox transition (8, 10, 14, 36) (Fig. 4).

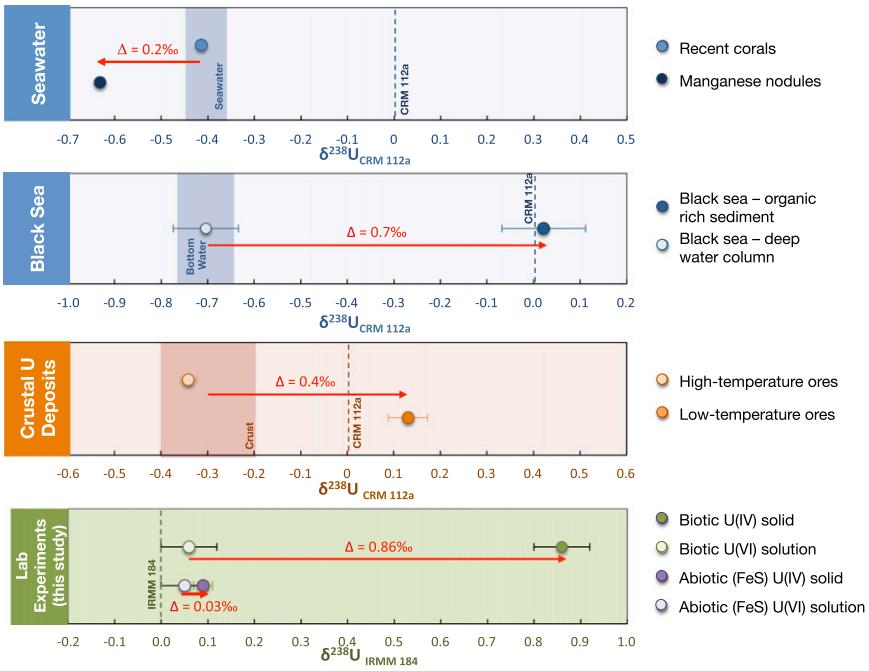

Fig. 4. Compilation of $\delta^{238}U$ values for various U(IV) deposits including seawater and authigenic U (blue) (9, 10, 14, 37) and crustal U deposits (orange) (8–10, 36) compared with biotic and abiotic reduction products (green and purple, this study). Red arrows indicate isotopic fractionation ($\Delta^{238}U$) between two products of U reduction. Symbols represent the mean of multiple samples, and the error bars represent the isotopic variation observed in each reservoir.

The results of this study suggest that, in many sedimentary deposits, enzymatic U reduction was a major driver for authigenic U enrichment, including marine sediments and shales (10, 14), as well as sandstone tabular and roll-front U deposits (8, 11, 36). For example, in the modern Black Sea, U isotope fractionation ($\Delta^{238}U$) of ~0.7‰ between the authigenic U in the sediment and that in the deep water column was observed (10, 13, 37). As the deep water column provides a maximum value for $\delta^{238}U$ of sediment pore water (12), this implies that U reduction in the sediment of euxinic basins is dominantly biotic.

U(VI) reduction is a relatively common biotic process, as it is carried out by varied metabolic groups of microorganisms—sulfate-reducing, iron-reducing, and fermenting bacteria among others (2)—and the biologically driven $^{238}U/^{235}U$ fractionation is consistent within these groups (17). Thus, the preferential accumulation of the heavy ^{238}U isotope in the solid U(IV) phase is a proxy for the presence and activity of metabolically diverse microorganisms in low-temperature sedimentary environments. Accordingly, the U isotope composition of the rock record may be specifically used as a "paleo-bioredox" proxy, rather than a conventional redox proxy, targeted to identify past environments in which redox processes were catalyzed biologically. The occurrence of heavy U isotope compositions in black shales and sandstone deposits, ranging in age from recent to late Archean (8–10, 14, 15, 36), indicates that bioreduction has been important ever since oxidized chemical species [i.e., U(VI)] became extant at the Earth's surface.

Methods

U Reduction Experiments. U reduction experiments (all but soluble sulfide) were conducted in duplicate in an anoxic chamber with an atmosphere of 2.5% H_2 and 97.5% N_2, using sterile serum bottles with a butyl rubber septum and anoxic solutions (30 mL). For the biotic cases, *Shewanella oneidensis* at an $OD_{600} = 1$ was inoculated either in a simple medium (BP; Table S1) or in a complex medium (WLP; Table S1) with 20 mM lactate as an electron donor. Previously reduced CFE was inoculated in BP medium in an amount equivalent to biomass of $OD_{600} = 1$. Because of the presence of 30 mM $NaHCO_3$, added U(VI) was present in solution predominantly as a uranyl-carbonate complex, $UO_2(CO_3)_3^{4-}$, as confirmed by aqueous speciation calculations (Fig. S5). Abiotic experiments were performed in a pH-buffered medium [containing 20 mM piperazine-*N,N′*-bis(2-ethanesulfonic) acid (Pipes) and 1 mM $NaHCO_3$ pH = 6.8], to which chemogenic FeS (at 1 or 5 mM final concentration), biogenic FeS (5 g/L final concentration), magnetite, green rust (5 mM as Fe final concentrations), peat (200 mg/L final concentration), or dissolved Fe(II) (5 mM final concentration) was added. U reduction was initiated by amending natural uranium [IRMM 184 standard (Institute for Reference Materials and Measurements) dissolved in the solution of 0.1 M HCl], yielding a final concentration between 50 and 100 mg/L.

Aliquots (0.3 mL) were withdrawn at time intervals and filtered through 0.22-μm membranes or 0.02-μm membranes in case of dissolved Fe(II), to quantify the remaining dissolved uranyl species in the filtrate. For chemogenic or biogenic FeS, magnetite, green rust, and peat experiments, U(VI) was quantitatively removed from solution, and a second type of sample was collected at the corresponding time points to quantify U(VI) remaining on the mineral phase. These subsamples were incubated overnight with $NaHCO_3$ (at a final concentration of 100 mM) to preferential desorb U(VI) by forming uranyl-carbonate complexes released into solution (5). Samples were withdrawn and filtered under strictly anoxic conditions to maintain U speciation. All collected samples were diluted in 0.1 M HNO_3 to an appropriate concentration for measurement by an ICP-MS. The results of monitoring U(VI) reduction are presented in Fig. 1. No isotopic effect was detected as a result of desorption.

Aqueous sulfide U(VI) reduction experiments were conducted in duplicate using serum bottles with butyl rubber septa and anoxic solutions as previously described (38). All bottles and solutions were thoroughly purged with ultra high purity He before initiation of the experiments to remove O_2. A 15-psi He overpressure was maintained throughout the experiments. A simple buffered medium consisting of 4.2 mM $NaHCO_3$, 12.5mM Tris-(hydroxymethyl)-aminomethane (Tris), and 4.2 mg/L U was prepared using a natural abundance U ICP solution as the starting U stock (Ricca PU1KN-100). A volume of 96 mL medium was degassed in a sealed serum bottle, and small aliquots of the medium were sampled via a He-purged syringe, and the pH of each bottle was adjusted to 6.75 ± 0.1 using dropwise addition of degassed dilute HCl. Experiments were initiated via the introduction of 4 mL of an anaerobic 50 mM NaHS solution (2 mM final concentration). At each time point, a 3-mL aliquot of solution was sampled via a He-flushed syringe through a 0.2-μm syringe filter to recover the residual dissolved U(VI). Following sampling, 10 mL concentrated HNO_3 was slowly passed through the filter to recover the solid phase U(IV). Following the experiment, both the dissolved and solid phase U subsamples were repeatedly digested with HNO_3/H_2O_2 to remove any organic or solid S(0) particles and prepared for isotopic analysis.

U Isotope Analysis. Uranium was purified using the chromatographic extraction method (based on Eichrom Uteva resin), as described previously (10). Before the ion-exchange chemistry, all samples were evaporated and treated by a mixture of 400 μL 32% H_2O_2 and 14 M HNO_3 (1:1) to remove any organic material. To an aliquot of about 400 ng U, which was used for MS analysis, an IRMM 3636-A $^{236}U/^{233}U$ double spike (10, 39) was added, to correct for isotope fractionation during purification and for instrumental mass discrimination during analyses with MC-ICP-MS (10).

U isotopic composition was measured with a Thermo Neptune MC ICP-MS at the Institute for Mineralogy at Leibniz Universität Hannover or the W. M. Keck Foundation Laboratory for Environmental Biogeochemistry at Arizona State University (ASU). For sample introduction, an ESI Apex nebulizer (without membrane) was coupled to the desolvation unit of a Cetac Aridus at Hannover, whereas an ESI Apex was used alone at ASU.

Samples were measured using a sample-standard bracketing method (i.e., every two samples were bracketed by double-spiked in-run isotopic standard). The in-run standard was either IRMM-184 at Hannover or CRM 145a (certified reference material) at ASU. IRMM-184 has an isotope composition of 137.68 (i.e., a value of $\delta\ ^{238}U = -1.16$ relative to the more commonly applied isotope standard CRM-112a) (39), and CRM-145a shares an isotopic composition with CRM-112a. The accuracy and precision were determined by replicate analyses of various U standards [REIMP 18A (Regular European Inter-Laboratory Measurement Evaluation Programme) and CRM-112A in Hannover and CRM-129A and an in house standard at ASU] during each session of sample analyses. The reproducibility of these standards was about 0.05‰ at Hannover and 0.1‰ at ASU (Table S7; all delta values there are reported relative to CRM-112A). The delta values for all standards used agree with those previously published (9, 11, 18, 19, 36) (Table S7).

Similar spike/sample ratios, corresponding to $^{236}U/^{235}U = 3$ in the spike-sample mix (within ±10%) were used for all samples and spiked in-run standard. The abundance sensitivity of the mass spectrometer was checked before and after each sample analysis session. It was used for a correction of the contribution from the tail of ^{238}U on mass 236, which was typically ≤0.1 ppm of the ^{238}U signal. Accordingly, the ratio of $^{238}U_{tail}/^{236}U_{spike}$ was typically ≤0.05‰. As we used no thorium for our experiments, a correction for the contribution of ^{232}ThH on ^{233}U was unnecessary.

ACKNOWLEDGMENTS. We thank the Stanford Synchrotron Radiation Lightsource (SSRL) Radiation Protection Group. We thank Kate Maher for helpful discussions. The work at École Polytechnique Fédérale de Lausanne was supported by Swiss National Science Foundation Grant 200020-144335. The extended X-ray absorption spectroscopy fine structure was carried out at SSRL, operated by Stanford University on behalf of the US Department of Energy (Basic Energy Science) and supported by SSRL Environmental Remediation Sciences Program and Biological and Environmental Research. The work in Hannover was supported by Annika Brüske and Alexandra Tangen. The work at Arizona Statue University was supported by the NASA Astrobiology Program and National Science Foundation Grant OCE-0952394 under the guidance of Ariel Anbar.

1. Beard BL, et al. (1999) Iron isotope biosignatures. *Science* 285(5435):1889–1892.
2. Wall JD, Krumholz LR (2006) Uranium reduction. *Annu Rev Microbiol* 60:149–166.
3. Borch T, et al. (2010) Biogeochemical redox processes and their impact on contaminant dynamics. *Environ Sci Technol* 44(1):15–23.
4. Goldhaber MB, Hemingway BS, Mohagheghi A, Reynolds RL, Northrop HR (1987) *Origin of Coffinite in Sedimentary Rocks by a Sequential Adsorption-Reduction Mechanism* (United States Geological Survey, Washington, DC), pp 131–144.
5. Veeramani H, et al. (2011) Products of abiotic U(VI) reduction by biogenic magnetite and vivianite. *Geochim Cosmochim Acta* 75(9):2512–2528.
6. Veeramani H, et al. (2013) Abiotic reductive immobilization of U(VI) by biogenic mackinawite. *Environ Sci Technol* 47(5):2361–2369.
7. Hyun SP, Davis JA, Sun K, Hayes KF (2012) Uranium(VI) reduction by iron(II) monosulfide mackinawite. *Environ Sci Technol* 46(6):3369–3376.
8. Brennecka GA, Borg LE, Hutcheon ID, Anbar AD (2010) Natural variations in uranium isotope ratios of uranium ore concentrates: Understanding the 238U/235U fractionation mechanism. *Earth Planet Sci Lett* 291(1-4):228–233.
9. Stirling CH, Andersen MB, Potter M, Halliday AN (2007) Low-temperature isotopic fractionation of uranium. *Earth Planet Sci Lett* 264(1-2):208–225.
10. Weyer S, et al. (2008) Natural fractionation of 238U/235U. *Geochim Cosmochim Acta* 72(2):345–359.
11. Murphy MJ, Stirling CH, Kaltenbach A, Turner SP, Schaefer BF (2014) Fractionation of U-238/U-235 by reduction during low temperature uranium mineralisation processes. *Earth Planet Sci Lett* 388:306–317.
12. Noordmann J, et al. (2015) Uranium and molybdenum isotope systematics in modern euxinic basins: Case studies from the central Baltic Sea and the Kyllaren fjord (Norway). *Chem Geol* 396(0):182–195.
13. Andersen MB, et al. (2014) A modern framework for the interpretation of U-238/U-235 in studies of ancient ocean redox. *Earth Planet Sci Lett* 400:184–194.
14. Montoya-Pino C, et al. (2010) Global enhancement of ocean anoxia during Oceanic Anoxic Event 2: A quantitative approach using U isotopes. *Geology* 38(4):315–318.
15. Kendall B, Brennecka G, Weyer S, Anbar AD (2013) Uranium isotope fractionation suggests oxidative uranium mobilization at 2.50 Ga. *Chem Geol* 362:105–114.
16. Brennecka GA, Herrmann AD, Algeo TJ, Anbar AD (2011) Rapid expansion of oceanic anoxia immediately before the end-Permian mass extinction. *Proc Natl Acad Sci USA* 108(43):17631–17634.
17. Basu A, Sanford RA, Johnson TM, Lundstrom CC, Löffler FE (2014) Uranium isotopic fractionation factors during U(VI) reduction by bacterial isolates. *Geochim Cosmochim Acta* 136(0):100–113.
18. Bopp CJ, 4th, et al. (2010) Uranium 238U/235U isotope ratios as indicators of reduction: Results from an *in situ* biostimulation experiment at Rifle, Colorado, U.S.A. *Environ Sci Technol* 44(15):5927–5933.
19. Schauble EA (2007) Role of nuclear volume in driving equilibrium stable isotope fractionation of mercury, thallium, and other very heavy elements. *Geochim Cosmochim Acta* 71(9):2170–2189.
20. Abe M, Suzuki T, Fujii Y, Hada M, Hirao K (2008) An ab initio molecular orbital study of the nuclear volume effects in uranium isotope fractionations. *J Chem Phys* 129(16):164309.
21. Marshall MJ, et al. (2006) c-Type cytochrome-dependent formation of U(IV) nanoparticles by *Shewanella oneidensis*. *PLoS Biol* 4(9):e268.
22. Bernier-Latmani R, et al. (2010) Non-uraninite products of microbial U(VI) reduction. *Environ Sci Technol* 44(24):9456–9462.
23. Scott KM, Lu X, Cavanaugh CM, Liu JS (2004) Optimal methods for estimating kinetic isotope effects from different forms of the Rayleigh distillation equation. *Geochim Cosmochim Acta* 68(3):433–442.
24. Fujii Y, Higuchi N, Haruno Y, Nomura M, Suzuki T (2006) Temperature dependence of isotope effects in uranium chemical exchange reactions. *J Nucl Sci Technol* 43(4):400–406.
25. Bigeleisen J (1996) Temperature dependence of the isotope chemistry of the heavy elements. *Proc Natl Acad Sci USA* 93(18):9393–9396.
26. Moynier F, Fujii T, Brennecka GA, Nielsen SG (2013) Nuclear field shift in natural environments. *C R Geosci* 345(3):150–159.
27. Wang X, Johnson TM, Lundstrom CC (2015) Isotope fractionation during oxidation of tetravalent uranium by dissolved oxygen. *Geochim Cosmochim Acta* 150(0):160–170.
28. Gorby YA, Lovley DR (1992) Enzymatic uranium precipitation. *Environ Sci Technol* 26(1):205–207.
29. Renock D, Mueller M, Yuan K, Ewing RC, Becker U (2013) The energetics and kinetics of uranyl reduction on pyrite, hematite, and magnetite surfaces: A powder microelectrode study. *Geochim Cosmochim Acta* 118:56–71.
30. Ilton ES, et al. (2010) Influence of dynamical conditions on the reduction of U(VI) at the magnetite-solution interface. *Environ Sci Technol* 44(1):170–176.
31. Singer DM, et al. (2012) U(VI) sorption and reduction kinetics on the magnetite (111) surface. *Environ Sci Technol* 46(7):3821–3830.
32. Skomurski FN, Ilton ES, Engelhard MH, Arey BW, Rosso KM (2011) Heterogeneous reduction of U6+ by structural Fe2+ from theory and experiment. *Geochim Cosmochim Acta* 75(22):7277–7290.
33. Latta DE, Gorski CA, Scherer MM (2012) Influence of Fe(2+)-catalysed iron oxide recrystallization on metal cycling. *Biochem Soc Trans* 40(6):1191–1197.
34. Rademacher LK, et al. (2006) Experimentally determined uranium isotope fractionation during reduction of hexavalent U by bacteria and zero valent iron. *Environ Sci Technol* 40(22):6943–6948.
35. Bargar JR, et al. (2013) Uranium redox transition pathways in acetate-amended sediments. *Proc Natl Acad Sci USA* 110(12):4506–4511.
36. Bopp CJ, Lundstrom CC, Johnson TM, Glessner JG (2009) Variations in 238U/235U in uranium ore deposits: Isotopic signatures of the U reduction process? *Geology* 37(7):611–614.
37. Romaniello SJ, Brennecka G, Anbar AD, Colman AS (2009) Natural isotopic fractionation of 238U/235U in the water column of the Black Sea. *EOS Trans AGU* 90(52).
38. Hua B, Xu H, Terry J, Deng B (2006) Kinetics of uranium(VI) reduction by hydrogen sulfide in anoxic aqueous systems. *Environ Sci Technol* 40(15):4666–4671.
39. Richter S, et al. (2010) New average values for the n(238U)/n(235U) isotope ratios of natural uranium standards. *Int J Mass Spectrom* 295(1–2):94–97.